Letter

Topological phase diagrams of in-plane field polarized Kitaev magnets

Li Ern Chern and Claudio Castelnovo
T.C.M. Group, Cavendish Laboratory, University of Cambridge, Cambridge CB3 0HE, United Kingdom

(Received 18 April 2023; accepted 30 April 2024; published 16 May 2024)

While the existence of a magnetic field induced quantum spin liquid in Kitaev magnets remains under debate, its topological properties often extend to proximal phases where they can lead to unusual behaviors of both fundamental and applied interests. Subjecting a generic nearest-neighbor spin model of Kitaev magnets to a sufficiently strong in-plane magnetic field, we study the resulting polarized phase and the associated magnon excitations. In contrast to the case of an out-of-plane magnetic field where the magnon band topology is enforced by symmetry, we find that it is possible for topologically trivial and nontrivial parameter regimes to coexist under in-plane magnetic fields. We map out the topological phase diagrams of the magnon bands, revealing a rich pattern of variation of the Chern number over the parameter space and the field angle. We further compute the magnon thermal Hall conductivity as a weighted summation of Berry curvatures, and discuss experimental implications of our results to planar thermal Hall effects in Kitaev magnets.

DOI: 10.1103/PhysRevB.109.L180407

Introduction. Recently, there have been tremendous efforts in the search for Kitaev spin liquid (KSL) [1] in candidate materials, ranging from iridates [2–4] and ruthenium halides [5–7] to cobaltates [8,9]. These so-called Kitaev magnets [10–13] may realize a dominant Kitaev interaction K via the Jackeli-Khaliullin [14] or related [15–17] mechanisms. Here, we focus on arguably the most popular among them, α-$RuCl_3$ [18], whose zero-field ground state is a zigzag (ZZ) magnetic order [19,20], due to the presence of other symmetry-allowed interactions than K [21]. However, an external magnetic field is found to promote a disordered phase, where a half-integer quantized thermal Hall conductivity $\kappa_{xy}^{2D}/T = (\nu/2)(\pi k_B^2/6\hbar)$ [22] is reported by Refs. [23–27], hinting at chiral Majorana edge modes with Chern number $\nu = \pm 1$ in a non-Abelian KSL [Figs. 1(a) and 1(b)]. It is also suggested that the field angle dependence of κ_{xy} [25] or heat capacity [28,29] can lend further support for the case of non-Abelian KSL. Meanwhile, other experiments [30,31] report that κ_{xy} in the field-induced phase behaves rather as a smooth function without any plateau, and decreases rapidly as the temperature approaches zero, which point to emergent heat carriers of bosonic nature.

While the existence of KSL at intermediate fields remains under debate [32–39], Kitaev magnets eventually polarize at sufficiently high fields, where the collective excitations are magnons, which can give rise to experimentally measurable transport signals. Furthermore, if the magnon bands are topological, the resulting thermal Hall conductivity can reach the same order of magnitude as the half quantized value [40–43]. Although for magnons κ_{xy} at low temperatures is not directly proportional to the Chern number ν of the lower band, the latter is very often a good indicator of the opposite sign of the former. Therefore, phase diagrams that reveal the magnon Chern number across generic model parameters of Kitaev magnets [44] are valuable to identify topological magnons and to interpret thermal transport measurements at high fields [Figs. 1(c) and 1(d)]. The main objective of this Letter is precisely to present such topological phase diagrams for in-plane magnetic fields, which are relevant to experiments of the planar thermal Hall effect [25,26,30,31,45].

We note that Kitaev magnets such as α-$RuCl_3$ are polarized more easily by in-plane fields than out-of-plane fields, likely due to an anisotropic g tensor [46–49] and a positive Γ interaction [50], which discounts the out-of-plane field strength and disfavors an out-of-plane magnetization, respectively [41,51]. The case of polarizing Kitaev magnets with strong out-of-plane fields has been studied theoretically in Ref. [52] (see also Ref. [53]). It is found that, within the linear spin-wave approximation, the $JK\Gamma\Gamma'$ model can be effectively reduced to a JK model. The C_3 symmetry also plays an important role in the diagnosis of magnon band topology in Kitaev magnets, based on topological quantum chemistry or symmetry indicator theory [54–58]. As demonstrated in Ref. [59], the magnon bands must be topological whenever a gap exists in between.

In this Letter, we consider the nearest-neighbor $JK\Gamma\Gamma'$ model polarized by in-plane magnetic fields, which break the C_3 symmetry, and map out the phase diagrams of topological magnons. Unlike the aforementioned case, none of the model parameters can be made redundant. We find that, as long as the field is not along the armchair direction, there exist parameter regions that are topological ($\nu = \pm 1$) as well as trivial ($\nu = 0$) ones, the latter of which can be understood via an effective Hamiltonian [52]. We discuss the implications of our results to thermal Hall conductivities of Kitaev magnets at high fields, from which we propose a scheme to determine the relevant candidate parametrizations.

Model. The most generic nearest-neighbor spin Hamiltonian for Kitaev magnets is the $JK\Gamma\Gamma'$ model [21]. In an external magnetic field $\mathbf{h}$, it reads

$$H = \sum_{\lambda=x,y,z} \sum_{\langle ij\rangle\in\lambda} \big[J\mathbf{S}_i\cdot\mathbf{S}_j + KS_i^\lambda S_j^\lambda + \Gamma\big(S_i^\mu S_j^\nu + S_i^\nu S_j^\mu\big) + \Gamma'\big(S_i^\mu S_j^\lambda + S_i^\lambda S_j^\mu + S_i^\nu S_j^\lambda + S_i^\lambda S_j^\nu\big)\big] - \sum_i \mathbf{h}\cdot\mathbf{S}_i, \quad (1)$$

where (λ,μ,ν) is a cyclic permutation of (x,y,z). For convenience of analysis, we write the field strength $|\mathbf{h}|\equiv hS$ in terms of the spin magnitude $S\equiv|\mathbf{S}_i|$ [60]. An in-plane field can be parametrized as $(h_a,h_b,h_c)=h(\cos\beta,\sin\beta,0)$, where $\beta\in[0,2\pi)$ is the azimuthal angle in the honeycomb plane [see Fig. 2(a)] [61]. We apply linear spin-wave theory [62,63] to the in-plane field polarized state of (1), and obtain an analytical expression for the magnon spectrum $\omega_\pm(\mathbf{k})=S\sqrt{E(\mathbf{k})\pm\Delta(\mathbf{k})}/2$, where

$$E(\mathbf{k}) = 4(h-c_1)^2 + |c_2f_\mathbf{k}+c_4g_\mathbf{k}|^2 - |c_5f_\mathbf{k}-c_4g_\mathbf{k}|^2 - 4|c_6(f_\mathbf{k}-3)+c_7g_\mathbf{k}|^2 + 2c_3(c_2+c_5)\mathrm{Re}[f_\mathbf{k}], \quad (2a)$$

$$\Delta^2(\mathbf{k}) = 16(h-c_1)^2|c_2f_\mathbf{k}+c_3+c_4g_\mathbf{k}|^2 - 4(c_2+c_5)^2\{\mathrm{Im}[f_\mathbf{k}(c_3+c_4g_\mathbf{k}^*)]\}^2 - 16\big(c_2^2-c_5^2\big)\{\mathrm{Im}[f_\mathbf{k}(3c_6-c_7g_\mathbf{k}^*)]\}^2 - 32(c_2+c_5)\mathrm{Im}[f_\mathbf{k}(3c_6-c_7g_\mathbf{k}^*)]\mathrm{Im}[c_6f_\mathbf{k}(c_3+c_4g_\mathbf{k}^*)+g_\mathbf{k}(c_3c_7+3c_4c_6)], \quad (2b)$$

$$c_1 = 3J+K-\Gamma-2\Gamma', \quad c_2 = \frac{1}{6}[12J+4K+2\Gamma+4\Gamma'+(K+2\Gamma-2\Gamma')\cos(2\beta)],$$
$$c_3 = -\frac{\cos(2\beta)}{2}(K+2\Gamma-2\Gamma'), \quad c_4 = \frac{\sin(2\beta)}{2\sqrt{3}}(K+2\Gamma-2\Gamma'), \quad c_5 = \Gamma+2\Gamma'-\frac{\cos(2\beta)}{6}(K+2\Gamma-2\Gamma'),$$
$$c_6 = \frac{\sin\beta}{3\sqrt{2}}(K-\Gamma+\Gamma'), \quad c_7 = \frac{\cos\beta}{\sqrt{6}}(K-\Gamma+\Gamma'), \quad (2c)$$

$f_\mathbf{k}=1+\exp(ik_1)+\exp(ik_2)$, $g_\mathbf{k}=\exp(ik_1)-\exp(ik_2)$, and $k_1,k_2\in[0,2\pi)$ are components of the crystal momentum defined according to $\mathbf{a}_1,\mathbf{a}_2$ in Fig. 2(a). Let $\Delta(\mathbf{k})=\sqrt{\Delta^2(\mathbf{k})}\geqslant 0$, so that $\omega_-(\mathbf{k})$ [$\omega_+(\mathbf{k})$] corresponds to the lower (upper) band. For clarity, we refer to the gap between the two bands, $\min_\mathbf{k}[\omega_+(\mathbf{k})-\omega_-(\mathbf{k})]\geqslant 0$, as the *band gap*, which is not to be confused with the *excitation gap*, $\min_\mathbf{k}\omega_-(\mathbf{k})>0$. Chern number is a topological invariant that can never change as long as a finite band gap is maintained [64], i.e., a topological phase transition can only occur when $\Delta(\mathbf{k})=0$ for some $\mathbf{k}$.

We assume a polarized state in which the excitation gap grows with h, so that the system becomes more stable as h increases, rather than undergoing a magnon instability. This requires $h>c_1$ [65], from which we deduce the following. For a given set of parameters $\{J,K,\Gamma,\Gamma'\}$, if the band gap is finite (zero), then it remains finite (zero) as h varies, unless $h\longrightarrow\infty$. Therefore, the topological phase diagrams are independent of the field strength, and, for a given field angle, we can map them out by first solving for the zeros of (2b) and then choosing a sufficiently high field to compute the Chern numbers [66–69] at parameters away from these zeros.

Topological phase diagrams. For finite in-plane fields, the band gap closes if and only if the set of parameters $\{J,K,\Gamma,\Gamma'\}$ meets any of the criteria listed in Table I. Whenever the band gap is finite, let the Chern number of the lower (upper) band be ν $(-\nu)$, which transforms according to the A_{2g} representation of the point group $\bar{3}m$ [70,71], and flips sign under time reversal [41], as in the case of the non-Abelian KSL [28]. More specifically, fixing the couplings, (i) $\nu\longrightarrow\nu$ if $\mathbf{h}$ is rotated by $2\pi/3$ about the out-of-plane axis, (ii) $\nu\longrightarrow-\nu$ if $\mathbf{h}$ is rotated by π about the b axis, and (iii) $\nu\longrightarrow-\nu$ if $\mathbf{h}\longrightarrow-\mathbf{h}$, while the phase boundaries are invariant under these actions [65]. Hence, $\beta\in[0,\pi/6]$ serves as an independent unit, to which all other angles can be related by symmetries [see Fig. 2(b)]. On the other hand, flipping the signs of all couplings leaves ν invariant [65].

For visualizations, we set $J=0$ and calculate ν over the spherical parameter space defined by $K^2+\Gamma^2+\Gamma'^2=1$, at the field angles $\beta=0,\pi/24,\pi/12,\pi/8,\pi/6$ [see Figs. 3(a)–3(f)] [72]. We make two observations, with the understanding that all angles mentioned below are defined modulo $\pi/3$. First, for $\beta\neq\pi/6$, there exist both parameter regions with topological magnons and those without. For $\beta=\pi/6$, topological magnons are altogether forbidden due to a C_2 symmetry [40,73]. Second, the total area A of the parameter regions with $\nu=\pm1$ is maximal at $\beta=0$, which implies that, for a Kitaev magnet dominated by nearest-neighbor anisotropic interactions, topological magnons are most likely found when the in-plane field is along the a axis [74].

To understand why magnons are topologically trivial in certain parameter regions, we analyze the linear spin-wave theory at high fields by systematically integrating out the pairing terms [52]. This is achieved via a Schrieffer-Wolff

TABLE I. For field angles $0\leqslant\beta<\pi/6$, the band gap closes if and only if the parameters of the $JK\Gamma\Gamma'$ model satisfy any of the following equations. For $\beta=\pi/6$, the band gap is zero whenever (I) or (4) is satisfied.

I	$K+2\Gamma-2\Gamma'=0$
II	$6J+2K+\Gamma+2\Gamma'=0$
III	$6J+2K+\Gamma+2\Gamma'+2(K+2\Gamma-2\Gamma')\cos(2\beta)=0$
IV	$6J+2K+\Gamma+2\Gamma'-2(K+2\Gamma-2\Gamma')\cos(2\beta+\pi/3)=0$
V	$6J+2K+\Gamma+2\Gamma'-2(K+2\Gamma-2\Gamma')\cos(2\beta-\pi/3)=0$
VI	$3J+K+2\Gamma+4\Gamma'=0$ if (4) holds
VII	$K-\Gamma+\Gamma'=0$ if (4) holds

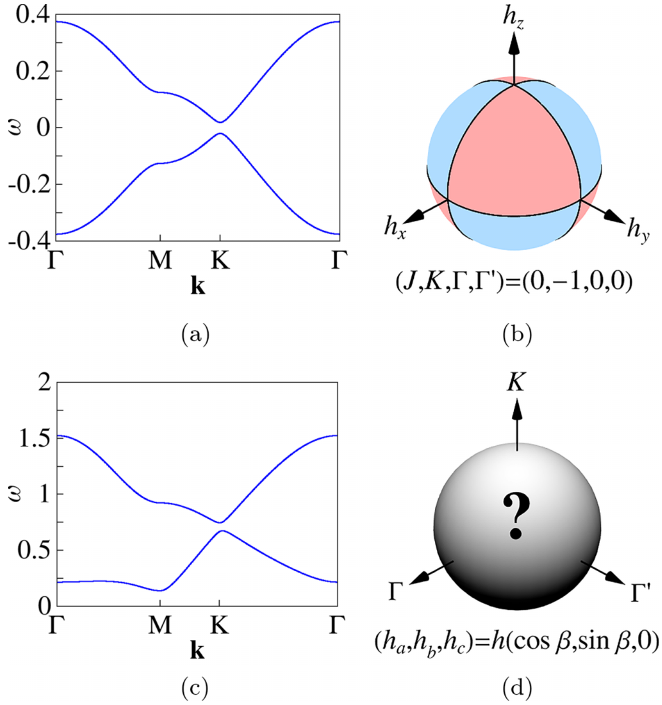

FIG. 1. (a) Majorana spectrum of Kitaev honeycomb model in a perturbative magnetic field. (b) For the non-Abelian KSL, the Chern number of the lower Majorana band depends on the field direction through $\nu = \mathrm{sgn}(h_x h_y h_z)$. Red (blue) areas indicate $\nu = +1$ (-1), while black curves indicate the vanishing of the band gap. (c) Magnon spectrum of the polarized state in a realistic spin model (1) of Kitaev magnets under a magnetic field. (d) For the in-plane field polarized state, we find a nontrivial variation of the magnon Chern number over the parameter space and the field angle [see Figs. 3(a)–3(f)].

transformation [75], from which we obtain an effective hopping model of the form $\mathcal{H}^{\text{eff}}(\mathbf{k}) = d_0(\mathbf{k})\mathbf{1}_{2\times 2} + \mathbf{d}(\mathbf{k})\cdot\boldsymbol{\sigma}$. The band gap vanishes if and only if $\mathbf{d}(\mathbf{k}) = \mathbf{0}$. When $\mathbf{d}(\mathbf{k}) \neq \mathbf{0}$, the Chern number of the lower band is given by the winding number of the map $\hat{\mathbf{d}}(\mathbf{k}) \equiv \mathbf{d}(\mathbf{k})/|\mathbf{d}(\mathbf{k})|$ from the Brillouin

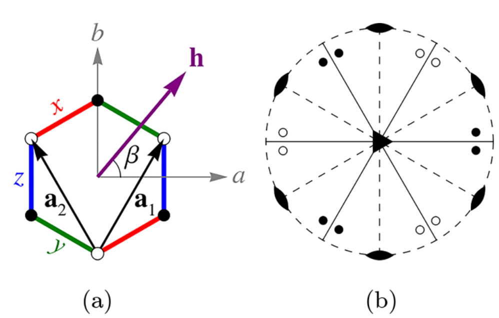

FIG. 2. (a) The three bond types x, y, and z in Kitaev magnets, the in-plane crystallographic axes a and b, and the primitive lattice vectors $\mathbf{a}_1$ and $\mathbf{a}_2$. An external magnetic field $\mathbf{h}$ is applied in-plane at the azimuthal angle β. (b) The $\bar{3}m$ point group of the $JK\Gamma\Gamma'$ model. If $\mathbf{h}$ transforms under a symmetry element that maps a solid circle to an open circle or vice versa, then the Chern number ν flips sign. If one circle is mapped to another of the same type, then ν remains invariant.

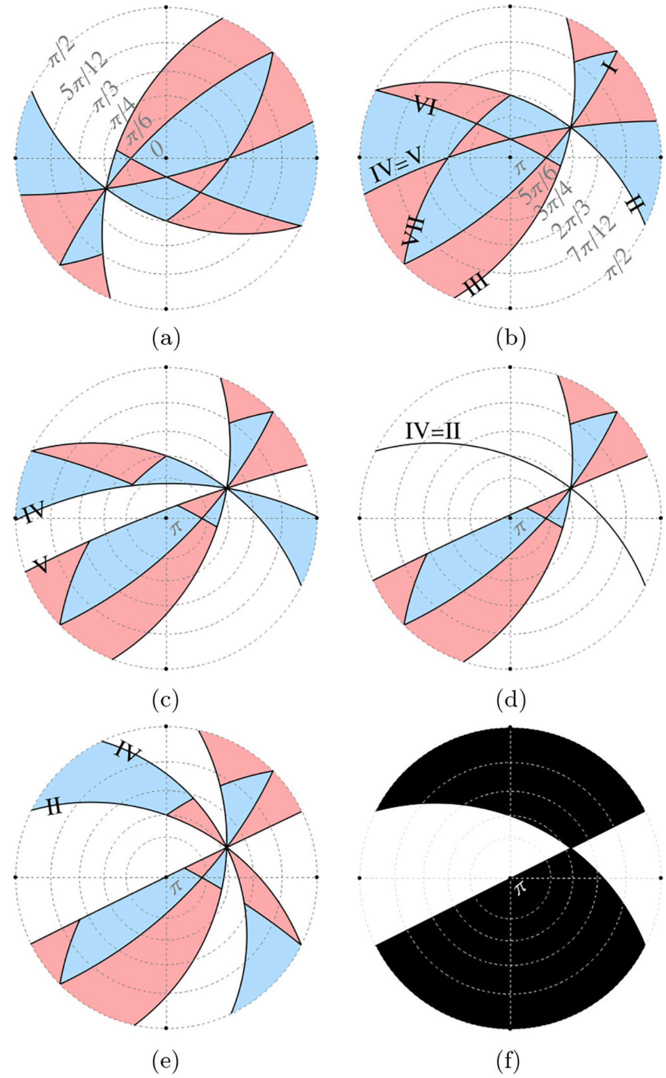

FIG. 3. Topological phase diagrams of the in-plane field polarized states at β equal to (a) 0, (b) 0, (c) $\pi/24$, (d) $\pi/12$, (e) $\pi/8$, and (f) $\pi/6$, over the space of couplings parametrized by $(J, K, \Gamma, \Gamma') = (0, \cos\theta, \sin\theta\cos\phi, \sin\theta\sin\phi)$. Red, white, and blue areas indicate the Chern number of the lower magnon band $\nu = +1$, 0, and -1, respectively, while black curves or areas indicate the vanishing of the band gap. Roman numerals label the phase boundaries as in Table I. Gray dashed circles indicate constant latitudes θ. In each diagram, the center is the $K = \pm 1$ ($\theta = 0$ or π) limit, while the left/right and top/bottom ends on the equator ($\theta = \pi/2$) are the $\Gamma = \pm 1$ ($\phi = 0$ or π) and $\Gamma' = \pm 1$ ($\phi = \pi/2$ or $3\pi/2$) limits, respectively.

zone to a sphere [66],

$$\nu = \frac{1}{4\pi}\int_{\text{FBZ}} \mathrm{d}^2\mathbf{k}\left[\hat{\mathbf{d}}(\mathbf{k})\cdot\frac{\partial\hat{\mathbf{d}}(\mathbf{k})}{\partial k_x}\times\frac{\partial\hat{\mathbf{d}}(\mathbf{k})}{\partial k_y}\right]. \tag{3}$$

One finds that the third component of $\mathbf{d}(\mathbf{k})$ vanishes throughout the Brillouin zone when $K - \Gamma + \Gamma' = 0$ [65], which defines the phase boundary (VII) within the parameter region

$$||c_2 + c_4| - |c_2 - c_4|| \leqslant |c_2 + c_3| \leqslant |c_2 + c_4| + |c_2 - c_4|. \tag{4}$$

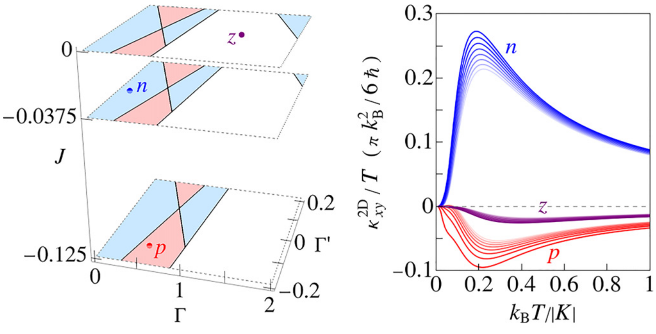

FIG. 4. (a) Candidate parametrizations p [82], n [83], and z [84] of α-$RuCl_3$, with K set to -1 and other interactions scaled accordingly, and topological phase diagrams in their neighborhoods under a magnetic field $\mathbf{h} \parallel a$. (b) Thermal Hall conductivities of p, n, and z due to magnons in the polarized state, at field strengths h starting from 0.18, 0.10, and 0.89, respectively, and increasing to 0.32, 0.24, and 1.03 in steps of 0.02. Lighter colors indicate higher fields. $S = 1/2$ is used.

On the other hand, there exist parameters outside (4) that satisfy $K - \Gamma + \Gamma' = 0$ and possess a finite band gap simultaneously [76]. At these parameters, the triple product in (3) is identically zero, and consequently $\nu = 0$. Any other parameter that can be continuously connected to these parameters without a gap closing must be topologically trivial as well.

Thermal Hall effect. We discuss how the topological phase diagrams relate to experimentally measurable quantities by connecting the Chern number to the thermal Hall conductivity [77], which is given by [78–80]

$$\kappa_{xy} = -\frac{k_B^2 T}{\hbar V} \sum_{n=1}^{\mathcal{N}} \sum_{\mathbf{k}\in \mathrm{FBZ}} c_2\left[g\left(\frac{\hbar\omega_{n\mathbf{k}}}{k_B T}\right)\right]\Omega_{n\mathbf{k}} \tag{5}$$

for magnons, where n is the band index ranging from 1 to $\mathcal{N} = 2$, $c_2(x) = \int_0^x dt\, \ln^2[(1+t)/t]$, $g(x) = 1/(e^x - 1)$, and $\Omega_{n\mathbf{k}}$ is the momentum space Berry curvature [65]. While the Chern number ν_n is given by the summation of $\Omega_{n\mathbf{k}}$ over $\mathbf{k}$, κ_{xy} is given by a weighted summation of $\Omega_{n\mathbf{k}}$ with *nonpositive* weights. Also, high-energy magnons contribute less to κ_{xy} than low-energy ones. Therefore, though κ_{xy} is not directly proportional to ν, one can very often use the latter to infer the sign of the former at low temperatures. More precisely, $\nu > 0$ ($\nu < 0$) means that there is an excess of positive (negative) Berry curvatures in the lower band, and by (5) the sign of κ_{xy} is expected to be opposite to ν [81]. On the other hand, $\nu = 0$ means that the net Berry curvature is zero, so κ_{xy} is generically small though not necessarily zero, and its sign is arbitrary.

We illustrate these ideas with three proposed parametrizations of α-$RuCl_3$ in the literature, $(J, K, \Gamma, \Gamma') = (-1, -8, 4, -1)$ [82], $(-1.5, -40, 5.3, -0.9)$ [83], and $(0, -6.8, 9.5, 0)$ [84], where energies are given in units of meV. For $\mathbf{h} \parallel a$, these parametrizations are located in the $\nu = +1, -1$, and 0 regimes, respectively, so we label them by p, n, and z [see Fig. 4(a)]. For each of them, we calculate κ_{xy} as a function of T at several values of h [see Fig. 4(b)]. We find that κ_{xy} is negative (positive) for p (n) as expected, while κ_{xy} for z is several times smaller. If we assume that the measured $\kappa_{xy} > 0$ in the field-induced phase under $\mathbf{h} \parallel -a$ in α-$RuCl_3$ [25] is indeed determined by a dominant magnon contribution, then p appears to be a more promising candidate parametrization. We also list three criteria that are conducive for a large magnon thermal Hall effect, which help us to understand the difference in κ_{xy} between the three parametrizations, as follows. (i) The bands are topological. (ii) The excitation gap is not too large, so that the lower band is thermally populated at low temperatures. (iii) The band gap is not too small, so that the population of the upper band remains negligible over an extended temperature range. For instance, at the respective lowest fields, the excitation gaps of p, n, and z are 0.16, 0.19, and 0.24, while the band gaps are 0.07, 0.25, and 0.78, in units of $|K|S$. n and p fulfill (i) and are comparable in (ii), but n does better than p in (iii), so n yields a larger κ_{xy}. On the other hand, z is comparable to p and n in (ii) and does better in (iii), but z fails (i), so its κ_{xy} is small. As h increases, the excitation gap becomes larger and κ_{xy} decreases.

Discussion. In summary, we have mapped out topological phase diagrams of Kitaev magnets polarized by in-plane magnetic fields, which reveal the magnon Chern number over a large parameter space. Since topological magnons are generally expected to yield a sizable thermal Hall conductivity with sign opposite to the Chern number at low temperatures, our results will be helpful in determining the relevant parametrizations of Kitaev magnets including α-$RuCl_3$. We briefly address the effects of the third-nearest-neighbor Heisenberg exchange [85,86] and the magnon interactions [87–94] in the Supplemental Material [65]. While the window of a field-induced KSL might be shut in many of the candidate materials, the door to topological magnons is most likely open and accessible via high fields. We appreciate that alternative sources of heat carriers in Kitaev magnets, such as spinons [95–97], triplons [98], phonons [99], and visons [100], as well as some effects arising from spin-lattice coupling [101–106], have been proposed. One particularly interesting future direction is to investigate the interplay between different types of topological excitations, whether they cooperate with one another and lead to a large thermal Hall conductivity [107] or other unusual properties.

Acknowledgments. We thank Kyusung Hwang, Hana Schiff, and Robert-Jan Slager for useful discussions. This work was supported by Engineering and Physical Sciences Research Council Grants No. EP/T028580/1 and No. EP/V062654/1.

[1] A. Kitaev, Anyons in an exactly solved model and beyond, Ann. Phys. **321**, 2 (2006).

[2] Y. Singh and P. Gegenwart, Antiferromagnetic Mott insulating state in single crystals of the honeycomb lattice material Na_2IrO_3, Phys. Rev. B **82**, 064412 (2010).

[3] Y. Singh, S. Manni, J. Reuther, T. Berlijn, R. Thomale, W. Ku, S. Trebst, and P. Gegenwart, Relevance of the Heisenberg-Kitaev model for the honeycomb lattice iridates A_2IrO_3, Phys. Rev. Lett. **108**, 127203 (2012).

[4] K. Kitagawa, T. Takayama, Y. Matsumoto, A. Kato, R. Takano, Y. Kishimoto, S. Bette, R. Dinnebier, G. Jackeli, and H. Takagi, A spin-orbital-entangled quantum liquid on a honeycomb lattice, Nature (London) **554**, 341 (2018).

[5] K. W. Plumb, J. P. Clancy, L. J. Sandilands, V. V. Shankar, Y. F. Hu, K. S. Burch, H.-Y. Kee, and Y.-J. Kim, α-$RuCl_3$: A spin-orbit assisted Mott insulator on a honeycomb lattice, Phys. Rev. B **90**, 041112(R) (2014).

[6] D. Ni, X. Gui, K. M. Powderly, and R. J. Cava, Honeycomb-structure RuI_3, a new quantum material related to α-$RuCl_3$, Adv. Mater. **34**, 2106831 (2022).

[7] Y. Imai, K. Nawa, Y. Shimizu, W. Yamada, H. Fujihara, T. Aoyama, R. Takahashi, D. Okuyama, T. Ohashi, M. Hagihala, S. Torii, D. Morikawa, M. Terauchi, T. Kawamata, M. Kato, H. Gotou, M. Itoh, T. J. Sato, and K. Ohgushi, Zigzag magnetic order in the Kitaev spin-liquid candidate material $RuBr_3$ with a honeycomb lattice, Phys. Rev. B **105**, L041112 (2022).

[8] R. Zhong, T. Gao, N. P. Ong, and R. J. Cava, Weak-field induced nonmagnetic state in a Co-based honeycomb, Sci. Adv. **6**, eaay6953 (2020).

[9] M. Songvilay, J. Robert, S. Petit, J. A. Rodriguez-Rivera, W. D. Ratcliff, F. Damay, V. Balédent, M. Jiménez-Ruiz, P. Lejay, E. Pachoud, A. Hadj-Azzem, V. Simonet, and C. Stock, Kitaev interactions in the Co honeycomb antiferromagnets $Na_3Co_2SbO_6$ and $Na_2Co_2TeO_6$, Phys. Rev. B **102**, 224429 (2020).

[10] S. M. Winter, A. A. Tsirlin, M. Daghofer, J. van den Brink, Y. Singh, P. Gegenwart, and R. Valentí, Models and materials for generalized Kitaev magnetism, J. Phys.: Condens. Matter **29**, 493002 (2017).

[11] H. Takagi, T. Takayama, G. Jackeli, G. Khaliullin, and S. E. Nagler, Concept and realization of Kitaev quantum spin liquids, Nat. Rev. Phys. **1**, 264 (2019).

[12] S. Trebst and C. Hickey, Kitaev materials, Phys. Rep. **950**, 1 (2022).

[13] S. Kim, B. Yuan, and Y.-J. Kim, α-$RuCl_3$ and other Kitaev materials, APL Mater. **10**, 080903 (2022).

[14] G. Jackeli and G. Khaliullin, Mott insulators in the strong spin-orbit coupling limit: From Heisenberg to a quantum compass and Kitaev models, Phys. Rev. Lett. **102**, 017205 (2009).

[15] H. Liu and G. Khaliullin, Pseudospin exchange interactions in d^7 cobalt compounds: Possible realization of the Kitaev model, Phys. Rev. B **97**, 014407 (2018).

[16] R. Sano, Y. Kato, and Y. Motome, Kitaev-Heisenberg Hamiltonian for high-spin d^7 Mott insulators, Phys. Rev. B **97**, 014408 (2018).

[17] H. Liu, J. Chaloupka, and G. Khaliullin, Kitaev spin liquid in 3d transition metal compounds, Phys. Rev. Lett. **125**, 047201 (2020).

[18] P. A. Maksimov and A. L. Chernyshev, Rethinking α-$RuCl_3$, Phys. Rev. Res. **2**, 033011 (2020).

[19] J. A. Sears, M. Songvilay, K. W. Plumb, J. P. Clancy, Y. Qiu, Y. Zhao, D. Parshall, and Y.-J. Kim, Magnetic order in α-$RuCl_3$: A honeycomb-lattice quantum magnet with strong spin-orbit coupling, Phys. Rev. B **91**, 144420 (2015).

[20] R. D. Johnson, S. C. Williams, A. A. Haghighirad, J. Singleton, V. Zapf, P. Manuel, I. I. Mazin, Y. Li, H. O. Jeschke, R. Valentí, and R. Coldea, Monoclinic crystal structure of α-$RuCl_3$ and the zigzag antiferromagnetic ground state, Phys. Rev. B **92**, 235119 (2015).

[21] J. G. Rau, E. K.-H. Lee, and H.-Y. Kee, Generic spin model for the honeycomb iridates beyond the Kitaev limit, Phys. Rev. Lett. **112**, 077204 (2014).

[22] $\kappa_{xy}^{2D} \equiv \kappa_{xy} d$ where d is the interlayer distance between the honeycomb planes in a three-dimensional structure.

[23] Y. Kasahara, T. Ohnishi, Y. Mizukami, O. Tanaka, S. Ma, K. Sugii, N. Kurita, H. Tanaka, J. Nasu, Y. Motome, T. Shibauchi, and Y. Matsuda, Majorana quantization and half-integer thermal quantum Hall effect in a Kitaev spin liquid, Nature (London) **559**, 227 (2018).

[24] M. Yamashita, J. Gouchi, Y. Uwatoko, N. Kurita, and H. Tanaka, Sample dependence of half-integer quantized thermal Hall effect in the Kitaev spin-liquid candidate α-$RuCl_3$, Phys. Rev. B **102**, 220404(R) (2020).

[25] T. Yokoi, S. Ma, Y. Kasahara, S. Kasahara, T. Shibauchi, N. Kurita, H. Tanaka, J. Nasu, Y. Motome, C. Hickey, S. Trebst, and Y. Matsuda, Half-integer quantized anomalous thermal Hall effect in the Kitaev material candidate α-$RuCl_3$, Science **373**, 568 (2021).

[26] J. A. N. Bruin, R. R. Claus, Y. Matsumoto, N. Kurita, H. Tanaka, and H. Takagi, Robustness of the thermal Hall effect close to half-quantization in α-$RuCl_3$, Nat. Phys. **18**, 401 (2022).

[27] Y. Kasahara, S. Suetsugu, T. Asaba, S. Kasahara, T. Shibauchi, N. Kurita, H. Tanaka, and Y. Matsuda, Quantized and unquantized thermal Hall conductance of the Kitaev spin liquid candidate α-$RuCl_3$, Phys. Rev. B **106**, L060410 (2022).

[28] K. Hwang, A. Go, J. H. Seong, T. Shibauchi, and E.-G. Moon, Identification of a Kitaev quantum spin liquid by magnetic field angle dependence, Nat. Commun. **13**, 323 (2022).

[29] O. Tanaka, Y. Mizukami, R. Harasawa, K. Hashimoto, K. Hwang, N. Kurita, H. Tanaka, S. Fujimoto, Y. Matsuda, E.-G. Moon, and T. Shibauchi, Thermodynamic evidence for a field-angle-dependent Majorana gap in a Kitaev spin liquid, Nat. Phys. **18**, 429 (2022).

[30] P. Czajka, T. Gao, M. Hirschberger, P. Lampen-Kelley, A. Banerjee, J. Yan, D. G. Mandrus, S. E. Nagler, and N. P. Ong, Oscillations of the thermal conductivity in the spin-liquid state of α-$RuCl_3$, Nat. Phys. **17**, 915 (2021).

[31] P. Czajka, T. Gao, M. Hirschberger, P. Lampen-Kelley, A. Banerjee, N. Quirk, D. G. Mandrus, S. E. Nagler, and N. P. Ong, Planar thermal Hall effect of topological bosons in the Kitaev magnet α-$RuCl_3$, Nat. Mater. **22**, 36 (2023).

[32] C. Hickey and S. Trebst, Emergence of a field-driven $U(1)$ spin liquid in the Kitaev honeycomb model, Nat. Commun. **10**, 530 (2019).

[33] N. D. Patel and N. Trivedi, Magnetic field-induced intermediate quantum spin liquid with a spinon Fermi surface, Proc. Natl. Acad. Sci. USA **116**, 12199 (2019).

[34] J. S. Gordon, A. Catuneanu, E. S. Sørensen, and H.-Y. Kee, Theory of the field-revealed Kitaev spin liquid, Nat. Commun. **10**, 2470 (2019).

[35] Y.-F. Jiang, T. P. Devereaux, and H.-C. Jiang, Field-induced quantum spin liquid in the Kitaev-Heisenberg model and its relation to α-$RuCl_3$, Phys. Rev. B **100**, 165123 (2019).

[36] J. Wang, B. Normand, and Z.-X. Liu, One proximate Kitaev spin liquid in the K-J-Γ model on the honeycomb lattice, Phys. Rev. Lett. **123**, 197201 (2019).

[37] L. E. Chern, R. Kaneko, H.-Y. Lee, and Y. B. Kim, Magnetic field induced competing phases in spin-orbital entangled Kitaev magnets, Phys. Rev. Res. **2**, 013014 (2020).

[38] H.-Y. Lee, R. Kaneko, L. E. Chern, T. Okubo, Y. Yamaji, N. Kawashima, and Y. B. Kim, Magnetic field induced quantum phases in a tensor network study of Kitaev magnets, Nat. Commun. **11**, 1639 (2020).

[39] M. Gohlke, L. E. Chern, H.-Y. Kee, and Y. B. Kim, Emergence of nematic paramagnet via quantum order-by-disorder and pseudo-Goldstone modes in Kitaev magnets, Phys. Rev. Res. **2**, 043023 (2020).

[40] L. E. Chern, E. Z. Zhang, and Y. B. Kim, Sign structure of thermal Hall conductivity and topological magnons for in-plane field polarized Kitaev magnets, Phys. Rev. Lett. **126**, 147201 (2021).

[41] E. Z. Zhang, L. E. Chern, and Y. B. Kim, Topological magnons for thermal Hall transport in frustrated magnets with bond-dependent interactions, Phys. Rev. B **103**, 174402 (2021).

[42] L. E. Chern, F. L. Buessen, and Y. B. Kim, Classical magnetic vortex liquid and large thermal Hall conductivity in frustrated magnets with bond-dependent interactions, npj Quantum Mater. **6**, 33 (2021).

[43] E. Z. Zhang, R. H. Wilke, and Y. B. Kim, Spin excitation continuum to topological magnon crossover and thermal Hall conductivity in Kitaev magnets, Phys. Rev. B **107**, 184418 (2023).

[44] F. Lu and Y.-M. Lu, Magnon band topology in spin-orbital coupled magnets: classification and application to α-$RuCl_3$, arXiv:1807.05232.

[45] H. Takeda, J. Mai, M. Akazawa, K. Tamura, J. Yan, K. Moovendaran, K. Raju, R. Sankar, K.-Y. Choi, and M. Yamashita, Planar thermal Hall effects in the Kitaev spin liquid candidate $Na_2Co_2TeO_6$, Phys. Rev. Res. **4**, L042035 (2022).

[46] Y. Kubota, H. Tanaka, T. Ono, Y. Narumi, and K. Kindo, Successive magnetic phase transitions in α-$RuCl_3$: XY-like frustrated magnet on the honeycomb lattice, Phys. Rev. B **91**, 094422 (2015).

[47] J. Chaloupka and G. Khaliullin, Magnetic anisotropy in the Kitaev model systems Na_2IrO_3 and α-$RuCl_3$, Phys. Rev. B **94**, 064435 (2016).

[48] R. Yadav, N. A. Bogdanov, V. M. Katukuri, S. Nishimoto, J. van den Brink, and L. Hozoi, Kitaev exchange and field-induced quantum spin-liquid states in honeycomb α-$RuCl_3$, Sci. Rep. **6**, 37925 (2016).

[49] S. M. Winter, K. Riedl, D. Kaib, R. Coldea, and R. Valentí, Probing α-$RuCl_3$ beyond magnetic order: Effects of temperature and magnetic field, Phys. Rev. Lett. **120**, 077203 (2018).

[50] J. A. Sears, L. E. Chern, S. Kim, P. J. Bereciartua, S. Francoual, Y. B. Kim, and Y.-J. Kim, Ferromagnetic Kitaev interaction and the origin of large magnetic anisotropy in α-$RuCl_3$, Nat. Phys. **16**, 837 (2020).

[51] L. E. Chern, Magnetic field induced phases in Kitaev magnets: A semiclassical analysis, Ph.D. thesis, University of Toronto, 2021.

[52] P. A. McClarty, X.-Y. Dong, M. Gohlke, J. G. Rau, F. Pollmann, R. Moessner, and K. Penc, Topological magnons in Kitaev magnets at high fields, Phys. Rev. B **98**, 060404(R) (2018).

[53] D. G. Joshi, Topological excitations in the ferromagnetic Kitaev-Heisenberg model, Phys. Rev. B **98**, 060405(R) (2018).

[54] H. C. Po, A. Vishwanath, and H. Watanabe, Symmetry-based indicators of band topology in the 230 space groups, Nat. Commun. **8**, 50 (2017).

[55] B. Bradlyn, L. Elcoro, J. Cano, M. G. Vergniory, Z. Wang, C. Felser, M. I. Aroyo, and B. A. Bernevig, Topological quantum chemistry, Nature (London) **547**, 298 (2017).

[56] J. Kruthoff, J. de Boer, J. van Wezel, C. L. Kane, and R.-J. Slager, Topological classification of crystalline insulators through band structure combinatorics, Phys. Rev. X **7**, 041069 (2017).

[57] H. Watanabe, H. C. Po, and A. Vishwanath, Structure and topology of band structures in the 1651 magnetic space groups, Sci. Adv. **4**, eaat8685 (2018).

[58] L. Elcoro, B. J. Wieder, Z. Song, Y. Xu, B. Bradlyn, and B. A. Bernevig, Magnetic topological quantum chemistry, Nat. Commun. **12**, 5965 (2021).

[59] A. Corticelli, R. Moessner, and P. A. McClarty, Identifying and constructing complex magnon band topology, Phys. Rev. Lett. **130**, 206702 (2023).

[60] We also take S to be dimensionless so that J, K, Γ, Γ' and h have units of energy.

[61] The crystallographic *abc* axes, which distinguish the in-plane and out-of-plane directions, and the cubic *xyz* axes, according to which the spin components in (1) are defined, are related by $a \parallel [11\bar{2}]$, $b \parallel [\bar{1}10]$, and $c \parallel [111]$.

[62] T. Holstein and H. Primakoff, Field dependence of the intrinsic domain magnetization of a ferromagnet, Phys. Rev. **58**, 1098 (1940).

[63] D. H. Jones, Q. A. Pankhurst, and C. E. Johnson, Spin-wave theory of anisotropic antiferromagnets in applied magnetic fields, J. Phys. C **20**, 5149 (1987).

[64] P. A. McClarty, Topological magnons: A review, Annu. Rev. Condens. Matter Phys. **13**, 171 (2022).

[65] See Supplemental Material at http://link.aps.org/supplemental/10.1103/PhysRevB.109.L180407 for details of linear spin-wave theory, computation of Chern number, symmetries, Schrieffer-Wolff transformation, third-nearest-neighbor Heisenberg exchange, and nonlinear spin-wave theory.

[66] B. A. Bernevig and T. L. Hughes, *Topological Insulators and Topological Superconductors* (Princeton University Press, NJ, 2013).

[67] D. Vanderbilt, *Berry Phases in Electronic Structure Theory* (Cambridge University Press, Cambridge, UK, 2018).

[68] T. Fukui, Y. Hatsugai, and H. Suzuki, Chern numbers in discretized Brillouin zone: Efficient method of computing (spin) Hall conductances, J. Phys. Soc. Jpn. **74**, 1674 (2005).

[69] C. Wang, H. Zhang, H. Yuan, J. Zhong, and C. Lu, Universal numerical calculation method for the Berry curvature and Chern numbers of typical topological photonic crystals, Front. Optoelectron. **13**, 73 (2020).

[70] C. Bradley and A. Cracknell, *The Mathematical Theory of Symmetry in Solids*, Oxford Classic Texts in the Physical Sciences (Oxford University Press, Oxford, UK, 1972).

[71] M. S. Dresselhaus, G. Dresselhaus, and A. Jorio, *Group Theory: Application to the Physics of Condensed Matter* (Springer, Berlin, 2008).

[72] We have used the stereographic projection $(\Gamma/(1 \pm K), \Gamma'/(1 \pm K))$, where the plus (minus) sign is for the $K > 0$ ($K < 0$) hemisphere.

[73] J. S. Gordon and H.-Y. Kee, Testing topological phase transitions in Kitaev materials under in-plane magnetic fields: Application to α-RuCl$_3$, Phys. Rev. Res. **3**, 013179 (2021).
[74] A plot of $A(\beta)$ is shown in the Supplemental Material [65].
[75] S. Bravyi, D. P. DiVincenzo, and D. Loss, Schrieffer-Wolff transformation for quantum many-body systems, Ann. Phys. **326**, 2793 (2011).
[76] One can imagine the extension of (VII) to the white areas in Figs. 3(a)–3(e).
[77] We assume that the heat current is applied along the *a* axis, while the transverse temperature gradient is measured along the *b* axis, as in the experiments.
[78] R. Matsumoto and S. Murakami, Theoretical prediction of a rotating magnon wave packet in ferromagnets, Phys. Rev. Lett. **106**, 197202 (2011).
[79] R. Matsumoto, R. Shindou, and S. Murakami, Thermal Hall effect of magnons in magnets with dipolar interaction, Phys. Rev. B **89**, 054420 (2014).
[80] S. Murakami and A. Okamoto, Thermal Hall effect of magnons, J. Phys. Soc. Jpn. **86**, 011010 (2017).
[81] There may be a situation where $\nu > 0$ but $\Omega_{n\mathbf{k}} < 0$ is concentrated at the lowest-energy magnons, so that κ_{xy} have the same sign as ν in a small temperature window near $T = 0$. However, if we examine an extended temperature range, we have predominantly $\mathrm{sgn}(\kappa_{xy}) = -\mathrm{sgn}(\nu)$.
[82] H.-S. Kim and H.-Y. Kee, Crystal structure and magnetism in α-RuCl$_3$: An *ab initio* study, Phys. Rev. B **93**, 155143 (2016).
[83] T. Suzuki and S.-I. Suga, Effective model with strong Kitaev interactions for α-RuCl$_3$, Phys. Rev. B **97**, 134424 (2018).
[84] K. Ran, J. Wang, W. Wang, Z.-Y. Dong, X. Ren, S. Bao, S. Li, Z. Ma, Y. Gan, Y. Zhang, J. T. Park, G. Deng, S. Danilkin, S.-L. Yu, J.-X. Li, and J. Wen, Spin-wave excitations evidencing the Kitaev interaction in single crystalline α-RuCl$_3$, Phys. Rev. Lett. **118**, 107203 (2017).
[85] S. M. Winter, Y. Li, H. O. Jeschke, and R. Valentí, Challenges in design of Kitaev materials: Magnetic interactions from competing energy scales, Phys. Rev. B **93**, 214431 (2016).
[86] S. M. Winter, K. Riedl, P. A. Maksimov, A. L. Chernyshev, A. Honecker, and R. Valentí, Breakdown of magnons in a strongly spin-orbital coupled magnet, Nat. Commun. **8**, 1152 (2017).
[87] A. L. Chernyshev and M. E. Zhitomirsky, Spin waves in a triangular lattice antiferromagnet: Decays, spectrum renormalization, and singularities, Phys. Rev. B **79**, 144416 (2009).
[88] M. E. Zhitomirsky and A. L. Chernyshev, Colloquium: Spontaneous magnon decays, Rev. Mod. Phys. **85**, 219 (2013).
[89] M. Mourigal, W. T. Fuhrman, A. L. Chernyshev, and M. E. Zhitomirsky, Dynamical structure factor of the triangular-lattice antiferromagnet, Phys. Rev. B **88**, 094407 (2013).
[90] P. A. Maksimov and A. L. Chernyshev, Field-induced dynamical properties of the *XXZ* model on a honeycomb lattice, Phys. Rev. B **93**, 014418 (2016).
[91] P. M. Cônsoli, L. Janssen, M. Vojta, and E. C. Andrade, Heisenberg-Kitaev model in a magnetic field: $1/S$ expansion, Phys. Rev. B **102**, 155134 (2020).
[92] R. Schick, O. Götze, T. Ziman, R. Zinke, J. Richter, and M. E. Zhitomirsky, Ground-state selection by magnon interactions in a fcc antiferromagnet, Phys. Rev. B **106**, 094431 (2022).
[93] P. A. Maksimov and A. L. Chernyshev, Easy-plane anisotropic-exchange magnets on a honeycomb lattice: Quantum effects and dealing with them, Phys. Rev. B **106**, 214411 (2022).
[94] C. A. Gallegos and A. L. Chernyshev, Magnon interactions in the quantum paramagnetic phase of CoNb$_2$O$_6$, Phys. Rev. B **109**, 014424 (2024).
[95] Y. H. Gao, C. Hickey, T. Xiang, S. Trebst, and G. Chen, Thermal Hall signatures of non-Kitaev spin liquids in honeycomb Kitaev materials, Phys. Rev. Res. **1**, 013014 (2019).
[96] Y. Teng, Y. Zhang, R. Samajdar, M. S. Scheurer, and S. Sachdev, Unquantized thermal Hall effect in quantum spin liquids with spinon Fermi surfaces, Phys. Rev. Res. **2**, 033283 (2020).
[97] I. S. Villadiego, Pseudoscalar $U(1)$ spin liquids in α-RuCl$_3$, Phys. Rev. B **104**, 195149 (2021).
[98] P. S. Anisimov, F. Aust, G. Khaliullin, and M. Daghofer, Nontrivial triplon topology and triplon liquid in Kitaev-Heisenberg-type excitonic magnets, Phys. Rev. Lett. **122**, 177201 (2019).
[99] E. Lefrançois, G. Grissonnanche, J. Baglo, P. Lampen-Kelley, J.-Q. Yan, C. Balz, D. Mandrus, S. E. Nagler, S. Kim, Y.-J. Kim, N. Doiron-Leyraud, and L. Taillefer, Evidence of a phonon Hall effect in the Kitaev spin liquid candidate α-RuCl$_3$, Phys. Rev. X **12**, 021025 (2022).
[100] X.-Y. Song and T. Senthil, Translation-enriched $\mathbb{Z}_2$ spin liquids and topological vison bands: Possible application to α-RuCl$_3$, arXiv:2206.14197.
[101] Y. Vinkler-Aviv and A. Rosch, Approximately quantized thermal Hall effect of chiral liquids coupled to phonons, Phys. Rev. X **8**, 031032 (2018).
[102] M. Ye, G. B. Halász, L. Savary, and L. Balents, Quantization of the thermal Hall conductivity at small Hall angles, Phys. Rev. Lett. **121**, 147201 (2018).
[103] M. Ye, R. M. Fernandes, and N. B. Perkins, Phonon dynamics in the Kitaev spin liquid, Phys. Rev. Res. **2**, 033180 (2020).
[104] H. Li, T. T. Zhang, A. Said, G. Fabbris, D. G. Mazzone, J. Q. Yan, D. Mandrus, G. B. Halász, S. Okamoto, S. Murakami, M. P. M. Dean, H. N. Lee, and H. Miao, Giant phonon anomalies in the proximate Kitaev quantum spin liquid α-RuCl$_3$, Nat. Commun. **12**, 3513 (2021).
[105] S. Li and S. Okamoto, Thermal Hall effect in the Kitaev-Heisenberg system with spin-phonon coupling, Phys. Rev. B **106**, 024413 (2022).
[106] S. Li, H. Yan, and A. H. Nevidomskyy, Magnons, phonons, and thermal Hall effect in candidate Kitaev magnet α-RuCl$_3$, arXiv:2301.07401.
[107] N. Li, R. R. Neumann, S. K. Guang, Q. Huang, J. Liu, K. Xia, X. Y. Yue, Y. Sun, Y. Y. Wang, Q. J. Li, Y. Jiang, J. Fang, Z. Jiang, X. Zhao, A. Mook, J. Henk, I. Mertig, H. D. Zhou, and X. F. Sun, Magnon-polaron driven thermal Hall effect in a Heisenberg-Kitaev antiferromagnet, Phys. Rev. B **108**, L140402 (2023).